Validation of GOES-7 to a Radiation Budget for April and July 1994 ARM/IOP Using ScaRaB/Meteor-3/7 Data

A. Trishchenko and Z. Li
Canada Centre for Remote Sensing
Ottawa, Ontario, Canada

Abstract

Data from the ScaRaB radiometer flown on board the Meteor-3/7 satellite were employed for validating a TOA Earth radiation budget product generated from GOES-7 for the Atmospheric Radiation Measurement (ARM) Program. Comparisons were made between coincident and collocated short-wave and long-wave radiative quantities derived from ScaRaB and GOES sensors over the Southern Great Plains (SGP) Cloud and Radiation Testbed (CART) site in Oklahoma, U.S.A., during April and July 1994. Calibrations for both visible and infrared window channels appear to be adequate, but narrow- to broad-band conversion of short-wave measurements suffers systematic errors. After correcting this shortcoming, the ratio of cloud radiative forcing (a measure of the impact of clouds on atmospheric absorption) derived from ARM measurements turns out to be 1.07. This is in conformity with radiative transfer models.

Introduction

Radiation budget at the top of the atmosphere (TOA) is an important boundary condition of the earth's climate system and is essential for studying the transfer of solar energy within the system. Thus, monitoring these changes is key to understanding the climate system and its dynamics at different spatial and temporal scales.

There have been several space missions dedicated to monitoring the TOA radiation budget (TRB). Most notable are the Nimbus-7 (Jacobowitz 1984), the Earth Radiation Budget Experiment (ERBE) (Barkstrom et al. 1986), the Scanner for Radiation Budget (ScaRaB) (Kandel et al. 1994) and the Clouds and the Earth's Radiant Energy System (CERES) (Wielicki et al. 1995). Notwithstanding, continuous observation of TRB over a long period of time has not been achieved. For example, since the ERBE scanners ceased functioning in 1990, there have been almost no radiation budget measurements of high spatial resolution, except for only one year of observation by the ScaRaB. The dearth of TRB data during this period hinders, among others, the ARM Program. Lack of direct TOA radiation measurements necessitates the creation of a surrogate TRB data set from GOES weather satellites (Minnis et al. 1995). These data are valuable to many ARM investigations and have been employed in addressing such critical issues as the cloud absorption anomaly (Imre et al. 1996). However, since the GOES visible narrow-band sensor was not calibrated, the quality of the inferred broad-band data may be open to question without a proper validation (Cess et al. 1996).

A validation is presented here of the GOES-based TRB data-set for the SGP CART site using ScaRaB measurements. Two major potential sources of uncertainty, calibration and narrow- to broad-band conversions are examined. The calibration issue was addressed by comparing coincident and collocated measurements in the narrow-band channels of non-calibrated GOES radiometer and calibrated ScaRaB radiometer. Narrow- to broad-band conversion is assessed by comparing the conversion relationships used in generating the TRB data from GOES and obtained from the ScaRaB narrow and broad-band measurements.

Radiometers

ScaRaB/METEOR-3/7

ScaRaB is a space mission conducted jointly by France, Russia and Germany (Kandel et al. 1994). The first ScaRaB was launched on board the Russian METEOR-3/7 satellite, and the second one is planned for 1997. ScaRaB/METEOR-3/7 operated from February 1994 through March 1995. The METEOR-3/7 satellite rotated ~1200 km above the Earth on a non-sunsynchronous orbit, with an 82.5° inclination angle. The total period of satellite orbit precession with respect to the Sun was approximately 7 months, during which ScaRaB provided measurements at all local solar times for both ascending and descending orbits. Table 1 delineates some parameters of the ScaRaB radiometer including its four channels: visible (VIS, 0.55-0.65 μm),

Table 1. Characteristics of ScaRaB radiometer.	
Parameter	**Value**
Number of channels	4
Spectral intervals: 1. Visible channel 2. Solar channel 3. Total channel 4. IR window channel	 0.55 - 0.65 µm 0.2 - 4 µm 0.2 - > 50 µm 10.5-12.5 µm
Scanning mode	cross track
Number of pixel per line	51
Cycle duration	6 sec
Pixel measurement time	62.5 msec
Field of view	48x48 mrad
Pixel size at nadir	60x60 km^2
Angular distance between pixels	1.95°
Scanning angle limits	± 49°

short-wave (SW, 0.2-4 µm), total (TOT, 0.2- > 50 µm) and infrared window (IRW, 10.5 -12.5 µm). The field-of-view (FOV) of a nadir ScaRaB pixel is about 60X60 km^2.

ScaRaB has an on-board calibration system using multiple sources. They include the black body (BB) simulators for channels 3 (LW part) and 4 (IR window) and 3 sets of lamps for channels 1 (VIS), 2 (SW) and 3 (SW part). The visible channel was calibrated once every two weeks with one lamp (L11). SW calibration was done twice a day with one lamp and twice a month with another lamp. SW part of the TOT channel was calibrated twice a month. The IR window channel and the LW part of the TOT channel were calibrated every 12 seconds. Comparison of the calibrations for the TOT channel with a BB and a lamp and for the SW channel with two lamps demonstrate that the accuracy of calibration is generally within 0.2-0.5%. It is less accurate for VIS channel but still within 1-2%.

The accuracy of ScaRaB flux data was also evaluated by comparing synchronous measurements from the Earth Radiation Budget Satellite (ERBS) wide-field-of-view (WFOV) radiometer and from the ScaRaB scanning radiometer (Bess et al. 1997). The agreement is remarkably close, the mean differences being within $0.76\ Wm^{-2}$ for SW and $0.55\ Wm^{-2}$ for LW at night and $3.8\ Wm^{-2}$ during daytime and the standard deviations being $5.5\ Wm^{-2}$ for SW and 1.9 and $2.3\ Wm^{-2}$ for nighttime and daytime LW measurements. The agreement is comparable to that between the ERBE scanner and non-scanner observations (Green et al. 1990).

VISSR/GOES-7

The Visible and Infrared Spin-Scan Radiometer (VISSR) aboard GOES-7 did not have onboard calibration for the visible channel. Calibration of the GOES visible measurements is usually based on an intercomparison with NOAA/AVHRR that is calibrated with reference to some stable targets such as deserts, or in comparison with radiative transfer calculations (Whitlock et al. 1990, Rossow et al. 1992 1995; Rao and Chen 1994, Minnis et al. 1995). GOES visible calibration is given by the following equation:

$$L = G D^2 - C, \qquad (1)$$

where L is radiance ($Wm^{-2}sr^{-1}$) and D is 8-bit digital count. Due to the lack of consensus on calibration, the values of gain (G) and offset (C) vary among users and are subject to change with time (Rossow et al. 1992 and 1995). This study tests primarily the new calibration used by Minnis et al. (1995). Unlike the visible channel, the GOES IRW channel has an on-board calibration. Therefore, the brightness temperature was derived following a nominal calibration that assumed central wave length 11.5 µm.

GOES data have a spatial nadir resolution of about 1 km for visible channel and 4 km for IRW channel. However, reduced resolution data of 0.5oX0.5o and 0.3oX0.3o latitude and longitude generated by Minnis et al. (1995) at the NASA Langley Research Centre for the ARM Program are used here.

Data

Data employed in this study cover April and July 1994. GOES-7 data were available via the WWW from the NASA Langley Research Centre. They include TRB, visible and broad-band albedos, IR window brightness temperature, cloud parameters, etc. 0.5°-resolution data are employed as they are more comparable to the FOV of ScaRaB pixel data. Data of the two latest versions of GOES archive released on August 29, 1996 and April 25, 1997 were analyzed for April 1994. For July 1994 we used the versions of May 6, 1996 and April 25 ,1997. The April data encompass an area of 10°X14° over the SGP CART site, whereas the July data cover a much smaller area of 2.5°X2.5°. The difference between previous and the latest version of data consist of calibration of GOES data for July and new narrow- to broad-band conversion for both months.

ScaRaB A2 data were matched to the GOES-7 data. A2 contains individual ScaRaB pixel measurements of the TOA radiance and irradiance, as well as scene identification and georeferencing information. Data from GOES and ScaRaB were matched under the following constraints:

1. observation time difference less than 15 minutes
2. distance between the centers of ScaRaB pixels and GOES grid cells less than 20 km
3. difference in solar zenith angle less than 2.5°.

After being matched, the data are subject to a series of corrections to account for discrepancies in spectral coverage, viewing geometry and scene identification.

Validation

Calibration

After data are matched and corrected, validation of calibration was done by comparing narrow-band measurements from ScaRaB and GOES-7. Comparisons of individual pixel/grid data are shown in Figure 1 for April 1994 for all

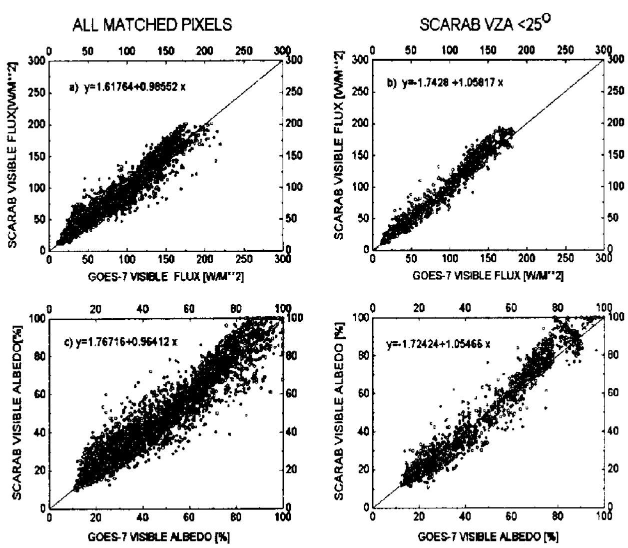

Figure 1. Comparison of visible fluxes (a and b) and albedos (c and d) from ScaRaB and GOES-7 for all matched data in April 1994 (a and c) and only those with the viewing zenith angle for ScaRaB less than 25°.

the matched data (left panels) and only those of comparable spatial resolutions between GOES-7 and ScaRaB data (right panels). The latter were obtained by restricting the VZAs of ScaRaB measurements less than 25° so that the FOVs of the ScaRaB data retained are less than 75 km.

The comparison of all matched data shows that there are good agreements in both albedos and fluxes, albeit large scattering. The mean difference is less that 2% in absolute albedo units. When the data of similar resolutions are compared, the scattering of the comparison is reduced and a small deviation from the 1:1 line is observed for larger albedo values. It should be pointed out that, due to the orbital constraints, the comparison shown in Figure 1 is limited to relatively low fluxes, given that the maximum potential value for reflected flux is about 300 W/m^2. This is partially because the minimum solar zenith angle for the matched data is around 40°. Average difference in albedo and fluxes in visible spectral band are summarized in Table 2.

Table 2. Average differences for albedos and fluxes. (GOES-7 data vs. April 26, 1997, ScaRaB VZA <25O).

Channel	Albedo [%]	Flux [Wm^{-2}]
Channel 1 Visible	0.4 ± 5.3	1.8 ± 8.3
Channel 2 Short-wave	0.3 ±4.7	2.1 ± 28.6

A comparison of brightness temperature during daytime (left panels) and nighttime (right panels) for April and July is shown in Figure 2. Good agreements are found for both daytime and nighttime comparisons. The scattering stems partially from match-up errors in space and time, and partially from an imperfect angular correction, in addition to a difference in spatial resolution. An additional comparison with a constraint that the viewing zenith angles of ScaRaB and GOES data do not differ by more than 5° shows even better agreement.

Broad-Band Data and Narrow- to Broad-Band Conversion

The GOES-based broad-band TOA fluxes were derived from narrow-band measurements following a narrow- to broad-band conversion. The performance of the conversion can be

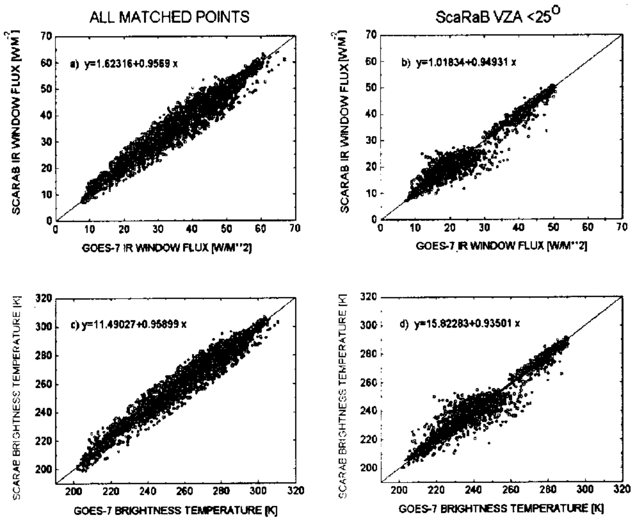

Figure 2. IR window fluxes (a and b) and brightness temperatures (c and d) for April and July observed during daytime (a and c) and nighttime (b and d). The linear fits to the data are also shown.

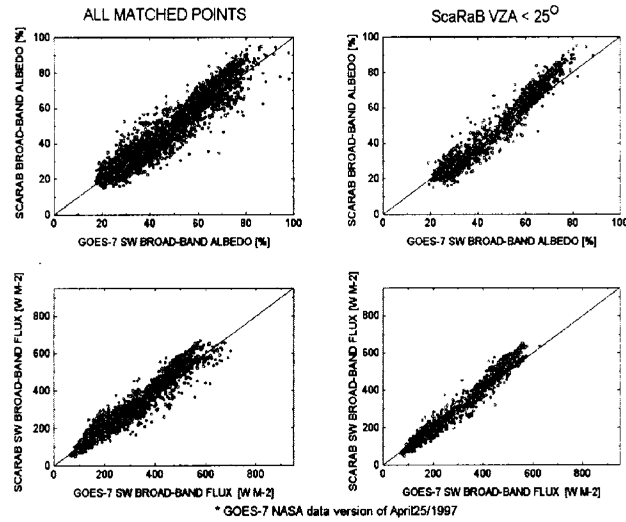

Figure 4. The same as Figure 3 but for updates GOES-7 data set.

evaluated by comparing broad-band albedos/fluxes estimated from GOES-7 and measured by ScaRaB. We analyzed two versions of GOES broad-band data products and found significant changes between versions. The results of comparison are shown in Figure 3 for a previous version of GOES data and in Figure 4 for a recently updated version.

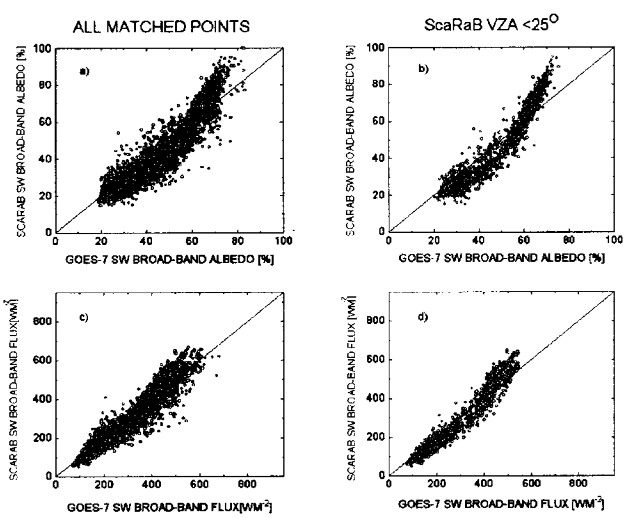

Figure 3. Short-wave broad-band albedo for April and July 1994 for GOES-7 data set released in August 1996.

The most striking feature of the short-wave albedo comparison is a curved trend deviated from 1:1 line, as is evident from Figure 3. The trend indicates that the GOES-based short-wave broad-band albedos were systematically lower than those measured by ScaRaB for highly reflective scenes (albedo > ~60%), and the opposite was the case for relatively dark scenes. The trend was less obvious for fluxes, because a large number of data points of high albedos were observed at low sun angles. This strong discrepancy was eliminated significantly in the recently updated version of GOES dataset. Average difference for SW albedo is 0.3± 4.7%. Average difference for fluxes is 2.1± 28.6Wm^{-2} for ScaRaB VZA <25° (Table 2).

The narrow- to broad-band conversion appears to dominate the discrepancy revealed here. To study the potential impact of solar zenith angle, data collected over an extended period (March-August 1994) were analyzed for each SZA interval of 10° in (Li and Trishchenko 1997). The broad-band albedo was found to be correlated linearly with visible albedo. The linearity of the relationship is consistent with many previous investigations (Minnis and Harrison 1984; Wydick et al. 1987; Li and Leighton 1992; Vesperini and Fouquart 1994; Hucek and Jacobowitz 1995). The slope and intercept of the linear regression depend moderately on the solar zenith angle, a new feature of the conversion that was not taken into account in previous studies. The conversion relationships used for generating the GOES-7 broad-band albedo are given below (Minnis et al. 1995).

$$\alpha_{sw} = \alpha_{sw}\,(CLR)\,(1-n) + \alpha_{sw}\,(CLD) * n \qquad (2)$$

$$\alpha_{sw}\,(CLR) = a_0 + a_1\,\alpha_v\,(CLR) + a_2 \ln(1/\mu_0) \qquad (3)$$

$$\alpha_{sw}\,(CLD) = b_0 + b_1\,\alpha_{VIS}\,(CLD) + b_2\,\alpha^2_{VIS}\,(CLD) + b_3 \ln(1/\mu 0) \qquad (4)$$

where n is cloud amount; CLR and CLD represent clear-sky and cloudy skies, respectively. The new version of narrow-to broad-band conversion applied to GOES-7 is similar to Eq. (4) but requires no discrimination between cloudy and clear scenes

$$\alpha_{sw} = 5.71 + 0.7198\,\alpha_{VIS} + 0.0287\,\alpha^2_{VI} + 5.23 \ln(1/\mu 0) \qquad (5)$$

Presumably, use of the quadratic equation is a major cause of the trend shown in Figure 3 and partly in Figure 4 in light of the linear relationship found by Li and Trishchenko (1997).

If the error of conversion is remedied, the TOA cloud radiative forcing (CRF) that is defined as the difference between all-sky and clear TOA net fluxes would increase in absolute magnitude and lead to a smaller surface to TOA cloud radiative forcing ratio (R),

$$R = CRF_{SFC} / CRF_{TOA} \qquad (6)$$

R has been employed in addressing the impact of cloud on atmospheric absorption (e.g., Cess et al. 1995; Imre et al. 1996). To quantify the impact of the conversion on the ratio, we computed R from the old and corrected according to ScaRaB regression GOES TOA SW broad-band fluxes for 6-30 April, 1994 excluding 13, 16, 20-21, 26-27. The selection of these data was based on the availability of surface measurements from the CERES/ARM/GEWEX Experiment (CAGEX) (Charlock and Alberta 1996). CAGEX compiled a comprehensive data base from a variety of ARM observation platforms for validating radiative transfer models. Scene identification needed for determining both surface and TOA CRF was based on the cloud amounts from GOES. From the old version of GOES-7 SW broad-band data, CRFTOA is found to be -189 Wm^{-2} and the corresponding CRFSFC obtained from CAGEX is -218 Wm^{-2}, leading to a R of 1.15. If the CRF_{TOA} is derived following the new narrow- to broad-band conversion, its value changes to -203 Wm^{-2}, a difference of 14 Wm^{-2}. Therefore, the new R is reduced from 1.15 to 1.07. Note that both numbers do not support the claim of cloud absorption anomaly for which R should be around 1.5 (Cess et al. 1995). An earlier version of the GOES-7 product was based on an incorrect calibration that led to larger value of R (>1.2) (Imre et al. 1996), which has been modified in the two latest releases.

The comparison of broad-band LW fluxes is presented in Figure 5 for all matched data (left panels) and those having similar VZAs with the same scenes identified by ScaRaB and GOES-7 (right panels). There seems to be no significant difference but a weak trend. GOES-7 technique tends to underestimate LW flux for warm scenes. The trend is, however, not very significant in comparison to the scattering of data points.

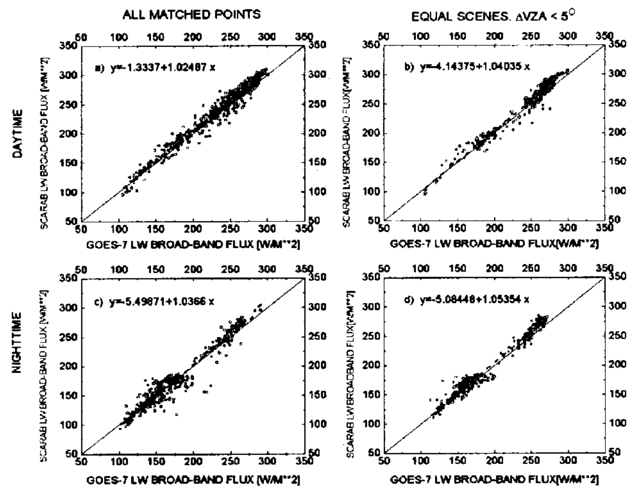

Figure 5. Comparisons of the long-wave broad-band fluxes observed by ScaRaB and estimated from GOES-7 IR window measurements during daytime (a and b) and nighttime (c and d) for all matched data (a and c) and only those of similar VZA (difference less than 5° with identical scene types determined by ScaRaB and GOES-7. Data from April and July 1994 were used.

Summary

This study validates two latest GOES-based TOA radiation data sets for April and July 1994 IOP generated for the ARM Program (Minnis et al. 1995). The validation was conducted by comparing with coincident and collocated narrow- and broad-band measurements made by the European ScaRaB. The comparisons have bearing on the quality of GOES calibration and narrow- to broad-band conversion which are the two major steps in converting GOES instrument counts into broad-band fluxes.

The data employed include visible and short-wave (SW) fluxes/albedos, infrared window (IRW) and long-wave (LW) fluxes/brightness temperatures obtained from VISSR/GOES-7 at grids of 0.5°X0.5° and ScaRaB of a nominal resolution 60 km. Comparisons were made between GOES-7 and ScaRaB in terms of fluxes, albedos and brightness temperatures. For narrow-band measurements in visible and infrared part of the spectrum, the two instruments agree well, except for a weak tendency that visible albedo/flux from ScaRaB are slightly larger over bright scenes. Comparison of SW broad-band data revealed that a previous version of the GOES-based estimates of albedos/fluxes suffered inaccurate narrow- to broad-band conversion. The conversion is linear according to ScaRaB visible and SW measurements, but a quadratic conversion relationship was employed in generating the GOES-based product. After removing this caveat, ScaRaB and GOES broad-band agree much better. Surface to TOA SW cloud radiative forcing ratio turns out to be 1.07 for April 1994 at the ARM CART site in Oklahoma after application of ScaRaB narrow-to broad-band conversion algorithm. This value is in perfect accordance with radiative transfer models.

Acknowledgments

We are indebted to the French Space Agency CNES for providing us with the main volume of ScaRaB data and R. Kandel, M. Viollier and P. Raberanto at Laboratoire de Meteorologie Dynamique du CNRS for making available the ScaRaB data of April 1994. A group of scientists led by P. Minnis at the NASA Langley Research Centre GOES-7 are gratefully acknowledged for generating the GOES product used in the study and for numerous discussions. Authors are also grateful to T. Charlock and T. Alberta for useful discussion and providing CAGEX data. The study was supported by the U.S. Department of Energy under an ARM grant DE-FG02-97ER2361.

References

Barkstrom, B. R. and G. L. Smith, 1986: The earth radiation budget experiment: science and implementation. *Rev. Geophys*., **24**, 379-390.

Bess, T. D., G. L. Smith, R. N. Green, D. A. Rutan, R. S. Kandel, P. Raberanto, and M. Viollier, 1997: Intercomparison of Scanning Radiometer for Radiation Budget (ScaRaB) and Earth Radiation Budget Experiment (ERBE) Results. *9th Conference on Atmospheric Radiation*. Long Beach, California, pp. 203-207.

Cess, R. D., M. H. Zhang, P. Minnis, L. Corsetti, E. G. Dutton, B. W. Forgan. D. P. Garber, W. L. Gates, J. J. Hack, E. F. Harrison, X. Jing, J. T. Kiehl, C. N. Long, J.-J. Moncrette, G. L. Potter, V. Ramanathan, B. Subasilar, C. H. Whitlock, D. F. Young, and Y. Zhou, 1995: Absorption of solar radiation by clouds: Observations versus models. *Science*, **267**, 496-499.

Cess, R. D., M. H. Zhang, Y. Zhou, X. Jing and V. Dvortsov, 1996: Absorption of solar radiation by clouds: Interpretation of satellite, surface, and aircraft measurements. *J. Geophys. Res*., **D101**, No. 18, 23299-23309.

Charlock, T. P., and T. L. Alberta, 1996: The CERES/ARM/GEWEX experiment (CAGEX) for the retrieval of radiative fluxes with satellite data. *Bull. Amer. Meteor. Soc*., **77**, 2673-2683.

Green, R. N., F. B. House. P. W. Stackhouse, X. Wu, S. A. Ackermann, W. L. Smith, and M. J. Johnson, 1990: Intercomparison of scanner and non-scanner measurements for the Earth Radiation Budget Experiment (ERBE). *J. Geophys. Res*., **95**, 11785-11798.

Hucek, R., and H. Jacobowitz, 1995: Impact of scene dependence on AVHRR Albedo models. *Journ. Atmos. Ocean. Technol*., **12**, 697-711.

Imre, D. G., E. H. Abramson, and P. H. Daum, 1996: Quantifying cloud-induced shortwave absorption: An examination of uncertainties and recent arguments for large excess absorption. *J. Appl. Meteor*., **35**, 1991-2010.

Jackobowitz, H., V. Soule, H. L. Kyle, F. B. House and the ERB Nimbus-7 experiment team, 1984: The Earth Radiation Budget (ERB) Experiment: An overview. *J. Geophys. Res*., **89**, 5021-5038.

Kandel, R. S., J-L. Monge, M. Viollier, L. A. Pakhomov, V. I. Adas'ko, R. G. Reitenbach, E. Raschke, and R. Stuhlmann, 1994: The ScaRaB Project: Earth radiation budget observations from meteor satellites. *Adv. Space Res*., **14**, 47-57.

Li, Z., and H. G. Leighton, 1992: Narrow-band to broad-band conversion with spatially autocorrelated reflectance measurements. *J Appl. Meteorol*., **31**, 421-432.

Li, Z., and A. Trishchenko, 1997: Narrow-to broad-band conversion: comparison of ScaRaB and GOES-7 measurements. *ARM Science Meeting Proceedings* (this issue).

Minnis, P., and E. F. Harrison, 1984: Diurnal variability of regional cloud and clear-sky radiative parameters derived from GOES data. Part III: November 1978 Radiative Parameters. *J. Clim and Appl. Meteor*., **23**, 1023-1051.

Minnis, P., W. L. Smith, D. P. Garber, J. K. Ayers, and D. R. Doelling, 1995: Cloud properties derived from GOES-7 for Spring 1994 ARM intensive observation period using version 1.0.0 of Arm Satellite Data Analysis Program. *NASA Reference Publication*, **1366**, 58 pp.

Rao, C.R.N., and J. Chen, 1994: Post-launch Calibration of the Visible and Near-Infrared Channels of the Advanced Very High Resolution Radiometers on NOAA-7,-9,11 Spacecraft. *NOAA Technical Report*. NESDIS, **78**, 22 pp.

Rossow, W. B., C. L. Brest., and M. D. Roiter, 1995: International Satellite Cloud Climatology Project (ISCCP). New radiance calibrations. *WMO/TD*. No **736**. World Meteorological Organization. 71 pp.

Rossow, W. B., Y. Desormeaux, C. L. Brest, and A. Parker, 1992: International Satellite Cloud Climatology Project (ISCCP). Radiance calibration report. *WMO/TD* No. **520**, WCRP-77. World Meteorological Organization. 104 pp.

Vesperini, M., and Y. Fouquart, 1994: Determination of broad-band shortwave fluxes from the Meteosat Visible Channel by comparison to ERBE. *Beitr. Phys. Atmosph*., **67**, N2, p. 121-131

Whitlock, C. H., W. F. Staylor, J. T. Suttles, G. L. Smith, R. Levin, R. Frouin, C. Gautier, P. M. Teillet, P. N. Slater, Y. J. Kaufman, B. N. Holben, W. B. Rossow, C. Brest, and S. R. LeCroy, 1990: AVHRR and VISSR satellite instrument calibration results for both cirrus and marine stratocumulus IFO periods. *FIRE Science Report* (NASA CP 3038).

Wielicki, B. A., B. Barkstrom, E. F. Harrison, R. B. Lee III, G. L. Smith, and J. E. Cooper, 1995: Clouds and the Earth's Radiant Energy System (CERES): An earth observing system experiment, *Bull. Amer. Meteor. Soc*., **76**, 853-868.

Wydick, J. E., P. A. Davis, and A. Gruber, 1987: Estimation of broad-band planetary albedo from operational narrow-band satellite measurements. *NOAA TR/NESDIS*, **27**, 32 pp.